

Emergent Superconductivity in the weak Mott insulator phase of bilayer Graphene Moiré Superlattice

Xiao-Chuan Wu,¹ Kelly Ann Pawlak,¹ Chao-Ming Jian,^{2,3} and Cenke Xu¹

¹*Department of Physics, University of California, Santa Barbara, CA 93106, USA*

²*Station Q, Microsoft Research, Santa Barbara, California 93106-6105, USA*

³*Kavli Institute of Theoretical Physics, Santa Barbara, CA 93106, USA*

(Dated: May 21, 2018)

We propose a phenomenological understanding of the recently discovered weak Mott insulator in the moiré superlattice of twisted bilayer graphene, especially the emergent superconductivity at low temperature within the weak Mott insulator phase, namely while lowering temperature, the longitudinal resistivity first grows below temperature T_m , but then rapidly drops to zero at even lower temperature T_c . An emergent superconductor in an insulator phase is very unusual. Here we propose that this phenomenon is due to the pure two-dimensional nature of the bilayer graphene moiré superlattice. We also compare our results with other theories proposed so far.

PACS numbers:

— Introduction

Recent discovery of superconductivity (SC) [1] near a weak Mott insulator (MI) phase in the graphene moiré superlattice [2, 3] sheds new light on our understanding of strongly correlated systems. This new system, with unprecedented tunability, is an ideal experimental platform to check our theoretical understandings. It is believed that the nearly flat mini bands of the system [4–7] play the major role in the most interesting phenomena observed so far. Within the recent theory works, Ref. 8, 9 described the system with an effective two-orbital extended Hubbard model on a triangular lattice near half-filling, the prediction of Ref. 8 has been checked with numerical methods [10]; Ref. 11–13 described the system with a tight binding model on a honeycomb lattice, while the electron Wannier functions strongly peak at the triangular lattice sites. The main difference between these two classes of models is that the latter models capture the physics related to Dirac band crossings between a *pair* of flat mini-bands. While at the doping where the SC and MI were observed, *i.e.* near half-filling within one of the mini-bands, it is not clear that any symmetry protected Dirac point away from the band plays a major role, unless one assumes a specific type of valley order, which leads to extra Dirac crossings within the mini flat band [11, 13]. But without compelling evidence of this particular valley ordering in the MI phase, the qualitative physics at the most relevant doping can potentially be captured by the (simpler) effective triangular lattice models introduced in Ref. 8, 9. Especially since the activation energy of the insulating phase is very low (4K) [2] even compared with the narrow bandwidth and the effective Hubbard interaction, this Mott insulator is rather weak and it is conceivable that its insulating behavior can be understood based solely on the electrons near the Fermi surface.

Nevertheless, the physics we discuss in the current work will be largely independent of the details of the mi-

croscopic model. We are going to focus on two peculiar and qualitative phenomena observed in Ref. 1.

(1) The resistivity $R_{xx}(T)$ in Ref. 1 shows that at the Mott insulator doping, $R_{xx}(T)$ first increases with lowering temperature below $T_m \sim 4-5\text{K}$ (as one would expect for an insulator), while rapidly drops to zero below another temperature scale $T_c \sim 1\text{K}$. This feature means that quite surprisingly the MI phase at very low energy scale still has a superconductivity instability.

(2) Once the SC is suppressed by a weak external magnetic field, the system becomes a normal MI with $R_{xx}(T)$ growing without saturation at low temperature.

As we have mentioned the insulator phase in this system must be a “weak” one, its activation gap is about the same as $k_B T_m$, which is much lower than the estimated Hubbard interaction, even with the large unit cell of the moiré structure. A weak Mott insulator can be naturally understood based on physics around the Fermi surface only. The electrons on the Fermi surface can be gapped out by an order parameter at finite momentum through folding of the Brillouin zone. When the amplitude of the order parameter is weak, *i.e.* when the system is close to the order-disorder quantum phase transition, only the “hot spots” on the Fermi surface connected by the momentum of the order parameter are gapped out; but with a sufficiently strong order parameter and its coupling to the electrons, the entire Fermi surface is gapped out, and the system becomes an insulator, which can usually be adiabatically connected to a strong Mott insulator at strong coupling without any phase transition.

The simplest analogue of the physics described above is the Hubbard model on the square lattice with nearest neighbor hopping at exactly half filling. A weak Hubbard interaction will induce the antiferromagnetic order at momentum (π, π) and drive the system into an insulator due to the Brillouin zone folding and nesting of Fermi surface. And the insulator with weak Hubbard U can be adiabatically connected to the insulator with large

U , where all the electrons are well localized on every site.

— *Mechanism for weak MI and emergent SC*

Ref. 8, 9 both started with a two orbital extended Hubbard model to understand the main experimental observations of the moiré superlattice of twisted bilayer graphene. The site of the triangular lattice is a patch of the bilayer graphene with AA stacking. The two effective orbitals correspond to the two valleys at the corners of the Brillouin zone of the original honeycomb lattice. Both models in Ref. 8, 9 have a $SU(4)$ symmetry at the leading order, and the $SU(4)$ symmetry is broken by other interactions such as the Hund’s interaction. Ref. 8, 9 chose a different sign for the Hund’s coupling, hence the former prefers a spin triplet and valley singlet on every triangular lattice site, while the latter prefers a spin singlet and valley order.

Here we first argue that the phenomena (1) and (2) mentioned above can be both naturally explained within the framework of Ref. 8. A Hund’s coupling chosen as Ref. 8 will favor the two electrons on every site in the Mott insulator phase to form a spin-1, with an antiferromagnetic coupling between neighboring sites. The frustrated nature of the triangular lattice will likely drive the system into a spin density wave order. Even if we start with a geometrically unfrustrated honeycomb lattice, the weakness of the Mott insulator will also generate further neighbor spin interaction and even multi-spin interactions which frustrate the collinear magnetic order, and may as well lead to a spin density wave (SDW). This SDW order connects different parts of the Fermi surface through Brillouin zone folding. Phenomenon (2) suggests that when a “competing order” is suppressed and the SDW is stabilized, the entire Fermi surface should be gapped out by the SDW, i.e. there is no residual Fermi pocket left at the Fermi surface, hence the amplitude of the SDW and its coupling to the electrons are sufficiently strong. But let us not forget that the system is purely two dimensional, hence with a full spin $SU(2)$ symmetry, the spins can never form a true long range order at infinitesimal temperature. This situation is different from a magnetic order close to its quantum critical point, in the sense that close to a quantum critical point, both the amplitude and direction of the magnetic order parameter will fluctuate strongly; while in our case the amplitude of the SDW does not fluctuate strongly, it is the direction of the order parameter that modulates over a long correlation length scale $\xi(T)$.

A finite but long correlation length $\xi(T)$ implies that within a thin momentum shell around the Fermi surface with $|\mathbf{p}-\mathbf{k}_F| < \Lambda(T) \sim \hbar/\xi(T)$, the fermions will not feel the background SDW order parameter with finite correlation length. Rather than demonstrate this effect by detailed calculations based on a microscopic model, one can visualize this effect by simply coarse-graining the system, until \hbar/ξ becomes the ultraviolet (UV) cut-off (thickness) of the momentum shell around the Fermi surface follow-

ing the standard renormalization group picture of Fermi surface [14], and within this shell the electrons only see a very short range correlated SDW, whose effects can be neglected. The electrons within the thin shell are still “active” and can transport electric charge, or even form Cooper pairs (Fig. 1); while the electrons outside this momentum shell will effectively view the background SDW as a true long range order, and hence are effectively “gapped out”. Based on the phenomenon (2), we know that the gap induced by the SDW is strong enough when the SDW is stabilized by an external field.

The active fermion density is proportional to the thickness of the momentum shell $\Lambda(T) \sim \hbar/\xi(T)$. The correlation length $\xi(T)$ of a SDW with a full $SU(2)$ spin symmetry can be estimated from the standard renormalization group calculation. Let us take the noncollinear SDW as an example, which happens very often in frustrated magnet (the experimental phenomena would also be consistent with a collinear SDW at finite momentum). A noncollinear SDW would break the entire $SO(3)$ spin rotation group. The standard way of describing such SDW is to parameterize its configuration manifold with two orthogonal vectors $\mathbf{n}_1, \mathbf{n}_2$. It is convenient to introduce a $SU(2)$ spinor field $z = (z_1, z_2)^t$ [15], and

$$\mathbf{n}_1 \sim \text{Re}[z^t i \sigma^y \sigma z], \quad \mathbf{n}_2 \sim \text{Im}[z^t i \sigma^y \sigma z] \quad (1)$$

$z = (z_1, z_2)^t$ are complex bosonic fields at certain momentum \mathbf{Q} , and subject to constraint $|z_1|^2 + |z_2|^2 = 1$. The two component complex field z_α lives in a target manifold: the three dimensional sphere S^3 , and it must couple to a \mathbb{Z}_2 gauge field [15], and when z_α condenses the ground state manifold is S^3/\mathbb{Z}_2 , which is identical to the ground state manifold of a noncollinear SDW.

The finite temperature physics of the SDW is well described by the nonlinear sigma model (NLSM) defined with the spinor z_α field:

$$Z = \int D z_\alpha(x) \exp \left(- \int d^2x \frac{1}{2g} \sum_\alpha |\nabla z_\alpha|^2 \right), \quad (2)$$

where $g = k_B T / \rho_s$, and again ρ_s is the spin stiffness at zero temperature. The 2nd order renormalization group (RG) equation of the coupling constant g is

$$\frac{dg}{d \ln l} = \frac{1}{\pi} g^2 + O(g^3). \quad (3)$$

For small g (low temperature), the correlation length scales as:

$$\xi(T) \sim a_0 \exp \left(\frac{\pi \rho_s}{k_B T} \right), \quad (4)$$

with an extra less important power-law function of T/ρ_s in the prefactor [16, 17]. a_0 is the lattice constant of the moiré superlattice, ρ_s is the spin stiffness at zero temperature. This means that the energy width of the

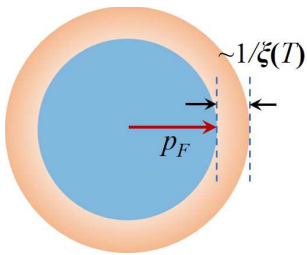


FIG. 1: The “active” electrons within the thin momentum shell around the Fermi surface with $|\mathbf{p} - \mathbf{p}_F| < \Lambda \sim \hbar/\xi(T)$, which are insensitive to the background SDW with finite correlation length $\xi(T)$, and hence can transport electric charge and potentially form a SC.

momentum shell $v_f\Lambda(T)$ is much smaller than the thermal energy $k_B T$ at low enough temperature T , hence the electrons in this shell are fully thermally excited. Thus the transport properties of these electrons can be captured by the most classical theory of transport, such as the Drude theory. For instance, the electric conductivity of the system is

$$\sigma(T) \sim \frac{n(T)e^2\tau}{m^*}, \quad (5)$$

where $n(T)$ is the density of electrons within this momentum shell, and it is proportional to $\Lambda(T)$. Thus we can see that although there is no true magnetic order at any finite temperature, due to the rapidly decreasing density of active electrons within the momentum shell, the resistivity $R_{xx}(T)$ will still rise with lowering temperature, before the system becomes a SC.

At low temperature, the active electrons within the momentum shell can still form a SC, which is consistent with the phenomenon (1) mentioned above. But since the correlation length $\xi(T)$ grows rapidly with lowering temperature, there are less and less active electrons available for pairing, which is a sign of strong competition between SC and the SDW. The SC transition temperature T_c for the active electrons can be estimated through the standard BCS theory, under the assumption of a uniform gap function around the Fermi surface (which is the case for almost all the superconductors predicted in this system so far):

$$\frac{1}{J} = \int_0^{v_f\Lambda(T)} d\varepsilon \frac{N}{\sqrt{\varepsilon^2 + \Delta^2}} \tanh\left(\frac{\sqrt{\varepsilon^2 + \Delta^2}}{k_B T}\right), \quad (6)$$

where J represents the Heisenberg interaction on the effective triangular lattice, which is the “gluing force” for superconductivity [8]. In Eq. 6 we have replaced the UV cut-off of the standard BCS theory by $v_f\Lambda(T)$. As always N is the density of states around the Fermi surface, which has been taken to be a constant. As we explained, at very low temperature $v_f\Lambda(T)$ is much smaller than

$k_B T$, hence at T_c ($\Delta = 0$), this equation can be simplified as

$$\frac{1}{NJ} = \frac{v_f\Lambda(T_c)}{k_B T_c}. \quad (7)$$

This equation does not always have a solution, it only supports a nonzero T_c when $NJ \gtrsim \pi\rho_s a_0/(\hbar v_f)$. Hence the system no longer has a BCS instability against infinitesimal attractive interaction, the interaction J needs to be stronger than a critical strength.

— *With weak anisotropy*

Once an external magnetic field is turned on (either inplane or out-of-plane), the magnetic order will be more “stabilized” at low temperature because the spin symmetry is reduced to $U(1)$, which supports a quasi long range order with infinite correlation length. In this case, the size of the momentum shell (and the density of the active electrons) vanishes to zero, and there is no room for SC.

The way a uniform Zeeman field couples to the spinor field z_α depends on the symmetry of the noncollinear SDW, but it will at least break the $SO(3)$ symmetry down to $U(1)$. A weak Zeeman field h will be renormalized to $h(l)$ at length scale l : $l/a_0 \sim (h(l)/h)^{1/\delta}$, where δ is the scaling dimension of h in the NLSM; while at the same length scale the coupling constant g is renormalized according to Eq. 3. Comparison between the RG flow of $h(l)$ and $g(l)$ defines a critical temperature T'_c :

$$\left(\frac{\rho_s}{h}\right)^{1/\delta} \sim \exp\left(\frac{\pi\rho_s}{k_B T'_c}\right). \quad (8)$$

When $T \ll T'_c$, the coupling constant $g(l)$ will still be small and perturbative when h becomes nonperturbative compared with ρ_s , hence $g(l)$ stops growing at a small value, and the system is in a quasi long range ordered SDW phase; while when $T \gg T'_c$, the coupling constant $g(l)$ becomes nonperturbative before $h(l)$ could affect the RG flow of Eq. 3, and the system is in the disordered phase. Thus T'_c can be viewed as the critical temperature of the $O(2)$ SDW (the Kosterlitz-Thouless transition critical temperature), which depends on the external Zeeman field h as

$$T'_c \sim \frac{\rho_s}{\log(\rho_s/h)}, \quad (9)$$

which is consistent with previous studies with magnetic systems with weak anisotropy [18].

As an illustration of the physics discussed above, let us consider a simple case without reflection symmetry (the reflection symmetry takes $z_\alpha \rightarrow \epsilon_{\alpha\beta} z_\beta^*$ in Ref. [15]), where an external field leads to the following anisotropic NLSM:

$$\int d^2x \frac{1}{2g_1} |\nabla z_1|^2 + \frac{1}{2g_2} |\nabla z_2|^2 + \frac{m^2}{k_B T} |z_1|^2, \quad (10)$$

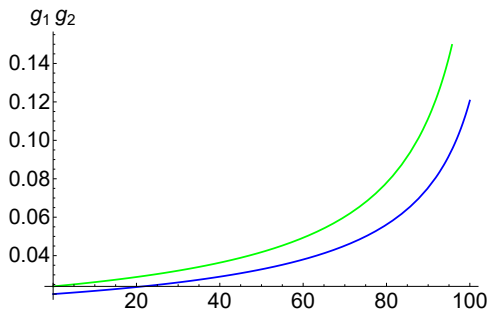


FIG. 2: The RG flow of g_1 and g_2 described by Eq. 12, with initial values $g_1 = 0.24$, $g_2 = 0.02$, and their difference is amplified under RG. The horizontal axis is the RG scale l .

$g_i = k_B T / \rho_i$. We take $\rho_2 > \rho_1$ for $m^2 > 0$, *i.e.* the anisotropy favors the condensate of z_2 , but penalizes condensate of z_1 .

Starting with $m = 0$, the RG flow of g_i is described by the Ricci flow [19, 20]:

$$\beta(g_{ab}) = -\frac{1}{2\pi} \mathcal{R}_{ab}, \quad (11)$$

where g_{ab} is the metric tensor of the target manifold of the NLSM, and \mathcal{R}_{ab} is the Ricci tensor (see appendix for more details). Expanded at the ordered state with $z_1 = 0$, $z_2 \neq 0$, the Ricci flow of the metric tensor translates into the RG flow of g_1 and g_2 in the field theory Eq. 10

$$\begin{aligned} \frac{dg_1}{d \ln l} &= \frac{1}{2\pi} \left(g_1^2 + \frac{g_1^3}{g_2} \right) + O(g_i^3), \\ \frac{dg_2}{d \ln l} &= \frac{1}{\pi} g_1 g_2 + O(g_i^3). \end{aligned} \quad (12)$$

The RG equations Ref. 12 can be solved exactly for arbitrary initial values of g_1 , g_2 with a complicated form (see appendix). If we start with a choice of different g_1 and g_2 , their difference will be amplified under RG flow (Fig. 2). Intuitively, as long as g_i are small enough (for low enough temperature or the spin stiffness is sufficiently strong), once m^2 is renormalized strong, z_1 will be explicitly gapped, and z_2 becomes an $O(2)$ order parameter, and enters a quasi long range algebraic phase where g_2 stops growing under RG. The general physics discussed in this section becomes manifest in model Eq. 10.

With increasing magnetic field h , the Mott insulator phase will eventually be destroyed, so will the SDW order. With strong field, the order-disorder transition of the SDW is likely a quantum phase transition with dynamical exponent 2, due to the precession of the inplane SDW order parameter under an external field.

— *Connections to more experimental phenomena, and comparison with other theories*

In our picture the weak Mott insulator is a consequence of a SDW at finite momentum, which significantly reduces the density of “active” fermions around the Fermi

surface with lowering temperature. Thus the SDW is a competing order of the SC. We expect this to be still true under small doping away from the Mott insulator. Experimentally the Hall density of charge carriers in the hole-doped Mott insulator is indeed proportional to the dopant density away from the Mott insulator, suggesting the persistence of the SDW under hole doping. And with an external field, either inplane or out-of-plane, the SDW will be stabilized (the effect of a weak magnetic field will be strongly amplified due to the logarithmic dependence of h in Eq. 9), thus the SC (even a spin triplet SC) will be significantly weakened due to its competition with the magnetic order.

We would also like to point out that the main phenomena (1) and (2) mentioned in the introduction are less likely to be simultaneously consistent with other theories proposed so far. Ref. 9 proposed a nematic order which spontaneously breaks the symmetry of the valley space in the Mott insulator phase, while Ref. 13 proposed a valence bond solid (VBS) order in the Mott insulator. The valley space does not have a $SU(2)$ symmetry, hence at low temperature it would form either a true long range order (which spontaneously breaks a discrete symmetry) or a quasi long range order (which spontaneously breaks the approximate $U(1)$ valley symmetry). In either case, it seems difficult to reconcile phenomena (1) and (2): since the system is clearly an insulator when the SC is suppressed, there must be no Fermi pockets left with the valley order; but the correlation length of the valley order remains infinite after the field is removed due to the lower symmetry of the valley space, hence the density of “active fermions” is still zero, and there seems no natural way to explain the emergence of SC inside the MI. The VBS order proposed in Ref. 13 has the similar issue.

— *Summary*

In summary we have proposed a phenomenological understanding of the unusual emergent superconductivity inside a weak Mott insulator observed recently in the bilayer Graphene Moiré superlattice. In our picture this peculiar phenomenon is due to the pure two dimensional nature of the system, and also the symmetry of the order parameter that leads to the MI. We expect this to be a quite generic mechanism, and similar behaviors can be found in other two dimensional systems.

CX is supported by the David and Lucile Packard Foundation. The authors thank Leon Balents, Charles Kane for very helpful discussions. While completing this paper, we became aware of an independent work [21] which aims to understand the same experimental phenomena.

[1] Y. Cao, V. Fatemi, S. Fang, K. Watanabe, T. Taniguchi, E. Kaxiras, and P. Jarillo-Herrero, Nature p.

- doi:10.1038/nature26160 (2018).
- [2] Y. Cao, V. Fatemi, A. Demir, S. Fang, S. L. Tomarken, J. Y. Luo, J. D. Sanchez-Yamagishi, K. Watanabe, T. Taniguchi, E. Kaxiras, et al., *Nature* p. doi:10.1038/nature26154 (2018).
- [3] G. Chen, L. Jiang, S. Wu, B. Lv, H. Li, K. Watanabe, T. Taniguchi, Z. Shi, Y. Zhang, and F. Wang, arXiv preprint arXiv:1803.01985 (2018).
- [4] R. Bistritzer and A. H. MacDonald, *Proceedings of the National Academy of Sciences* **108**, 12233 (2011), ISSN 0027-8424, <http://www.pnas.org/content/108/30/12233.full.pdf>, URL <http://www.pnas.org/content/108/30/12233>.
- [5] E. Suárez Morell, J. D. Correa, P. Vargas, M. Pacheco, and Z. Barticevic, *Phys. Rev. B* **82**, 121407 (2010), URL <https://link.aps.org/doi/10.1103/PhysRevB.82.121407>.
- [6] S. Fang and E. Kaxiras, *Phys. Rev. B* **93**, 235153 (2016), URL <https://link.aps.org/doi/10.1103/PhysRevB.93.235153>.
- [7] G. Trambly de Laissardière, D. Mayou, and L. Magaud, *Phys. Rev. B* **86**, 125413 (2012), URL <https://link.aps.org/doi/10.1103/PhysRevB.86.125413>.
- [8] C. Xu and L. Balents, arXiv:1803.08057 (2018).
- [9] J. F. Dodaro, S. A. Kivelson, Y. Schattner, X.-Q. Sun, and C. Wang, arXiv:1804.03162 (2018).
- [10] M. Fidrysiak, M. Zegrodnik, and J. Spalek, arXiv:1805.01179 (2018).
- [11] H. C. Po, L. Zou, A. Vishwanath, and T. Senthil, arXiv:1803.09742 (2018).
- [12] N. F. Q. Yuan and L. Fu, arXiv:1803.09699 (2018).
- [13] X. Y. Xu, K. T. Law, and P. A. Lee, arXiv:1805.00478 (2018).
- [14] R. Shankar, *Rev. Mod. Phys.* **66**, 129 (1994), URL <https://link.aps.org/doi/10.1103/RevModPhys.66.129>.
- [15] A. V. Chubukov, S. Sachdev, and T. Senthil, *Nuclear Physics B* **426**, 601 (1994), ISSN 0550-3213, URL <http://www.sciencedirect.com/science/article/pii/055032139490023X>.
- [16] P. Hasenfratz and F. Niedermayer, *Physics Letters B* **268**, 231 (1991), ISSN 0370-2693.
- [17] S. Sachdev, *Quantum Phase Transitions* (Cambridge University Press, 2011).
- [18] S. Hikami and T. Tsuneto, *Progress of Theoretical Physics* **63**, 387 (1980).
- [19] D. Friedan, *Phys. Rev. Lett.* **45**, 1057 (1980), URL <https://link.aps.org/doi/10.1103/PhysRevLett.45.1057>.
- [20] D. H. Friedan, *Annals of Physics* **163**, 318 (1985), ISSN 0003-4916, URL <http://www.sciencedirect.com/science/article/pii/0003491685903847>.
- [21] H. Isobe, N. F. Q. Yuan, and L. Fu, arXiv:1805.06449 (2018).

Appendix: From Ricci flow to RG equation

In this appendix, we discuss the effect of anisotropy on the noncollinear spin density wave from a geometric point of view. As we argued in the main text, the ground state manifold of the noncollinear spin density wave is a three dimensional manifold, which will be deformed by the Zeeman field. Thus the noncollinear spin density wave can be generally described by the NLSM

$$\mathcal{S}[X] = \int \frac{1}{2} G_{ab}[X] dX^a \wedge \star dX^b + \dots \quad (13)$$

where the bosonic field X is introduced as

$$\begin{pmatrix} X^1 \\ X^2 \\ X^3 \\ \sqrt{1 - |X|^2} \end{pmatrix} = \begin{pmatrix} \text{Re}z_1 \\ \text{Im}z_1 \\ \text{Re}z_2 \\ \text{Im}z_2 \end{pmatrix}, \quad (14)$$

and the metric G_{ab} should carry the information of the external Zeeman field which lowers the symmetry of the system. In our choice here, $X_i = 0$ corresponds to the ground state $|z_1|^2 = 0, |z_2|^2 = 1$.

To describe the geometric evolution of the target manifold more precisely, we need to introduce our conventions of geometric quantities. The affine connection is defined as

$$\Gamma^a_{bc} = \frac{1}{2} G^{ae} (-\partial_e G_{bc} + \partial_c G_{be} + \partial_b G_{ce}), \quad (15)$$

where $\partial_a = \frac{\partial}{\partial X^a}$ is the derivative with respect to the field X_i . This connection gives the Riemann curvature

$$R^a_{bcd} = \partial_c \Gamma^a_{db} - \partial_d \Gamma^a_{cb} + \Gamma^a_{ce} \Gamma^e_{db} - \Gamma^a_{de} \Gamma^e_{cb}, \quad (16)$$

and its contraction

$$\mathcal{R}_{ab} = R^c_{acb} \quad (17)$$

is called the Ricci tensor. The action Eq. 13 is invariant under coordinate transformations which preserve the distance $G_{ab} dX^a dX^b$.

Friedan [19, 20] proved that the one-loop beta function of G_{ab} corresponds to the Ricci flow

$$\frac{dG_{ab}}{d \ln l} = -\frac{1}{2\pi} \mathcal{R}_{ab} + \dots \quad (18)$$

Then the central task is to explore how the external Zeeman field affects the Ricci flow. Let us first consider the simpler case without the Zeeman field. The metric G_{ab} obtained from the isotropic O(4) NLSM reads

$$G_{ab}[X] = \frac{1}{g} \left(\delta_{ab} + \frac{X^a X^b}{1 - |X|^2} \right), \quad (19)$$

The Ricci tensor is given by

$$\mathcal{R}_{ab}[X] = 2g G_{ab}[X], \quad (20)$$

which is proportional to the metric. Using Eq. 18, we obtain the RG flow Eq. 3 of the coupling constant g .

After turning on the Zeeman term, the O(4) symmetry is broken, and the NLSM is modified as Eq. 10. The metric now becomes

$$G_{ab}[X] = \begin{pmatrix} \frac{1}{g_1} & 0 & 0 \\ 0 & \frac{1}{g_1} & 0 \\ 0 & 0 & \frac{1}{g_2} \end{pmatrix} + \frac{1}{g_2} \frac{X^a X^b}{1 - |X|^2}. \quad (21)$$

The complete expression of the Ricci tensor in this case is rather complicated. To read the RG flow of g_1, g_2 from the Ricci flow, we consider the Ricci tensor at point $X_i = 0$, which corresponds to the ordering of z_2 at zero temperature, and it is the order favored by the Zeeman field:

$$\mathcal{R}_{ab}[X \rightarrow 0] = \begin{pmatrix} 1 + \frac{g_1}{g_2} & 0 & 0 \\ 0 & 1 + \frac{g_1}{g_2} & 0 \\ 0 & 0 & \frac{2g_1}{g_2} \end{pmatrix}. \quad (22)$$

Combining with the value of $G_{ab}[X]$ at $X_i = 0$, we obtain the RG flow Eq. 12 of g_1 and g_2 .

If we start with initial values $g_1 = g$ and $g_2 = (1 - \alpha)g$, the solution of the RG equation Eq. 12 reads

$$\begin{aligned} g_1(l) &= \frac{\pi g}{\pi - g \ln l} \\ &+ \frac{g\pi^{3/2} \left(-\pi + g \ln l + \sqrt{\pi(\pi - g \ln l)} \right) \alpha}{(\pi - g \ln l)^{5/2}} + O(\alpha^2), \\ g_2(l) &= \frac{\pi g}{\pi - g \ln l} \\ &+ \frac{g \left(\pi^2 - 2\pi^{3/2} \sqrt{\pi - g \ln l} \right) \alpha}{(\pi - g \ln l)^2} + O(\alpha^2). \end{aligned} \quad (23)$$

-
- [1] Y. Cao, V. Fatemi, S. Fang, K. Watanabe, T. Taniguchi, E. Kaxiras, and P. Jarillo-Herrero, Nature p. doi:10.1038/nature26160 (2018).
 [2] Y. Cao, V. Fatemi, A. Demir, S. Fang, S. L. Tomarken, J. Y. Luo, J. D. Sanchez-Yamagishi, K. Watanabe, T. Taniguchi, E. Kaxiras, et al., Nature p. doi:10.1038/nature26154 (2018).
 [3] G. Chen, L. Jiang, S. Wu, B. Lv, H. Li, K. Watanabe, T. Taniguchi, Z. Shi, Y. Zhang, and F. Wang, arXiv preprint arXiv:1803.01985 (2018).

- [4] R. Bistritzer and A. H. MacDonald, Proceedings of the National Academy of Sciences **108**, 12233 (2011), ISSN 0027-8424, <http://www.pnas.org/content/108/30/12233.full.pdf>, URL <http://www.pnas.org/content/108/30/12233>.
 [5] E. Suárez Morell, J. D. Correa, P. Vargas, M. Pacheco, and Z. Barticevic, Phys. Rev. B **82**, 121407 (2010), URL <https://link.aps.org/doi/10.1103/PhysRevB.82.121407>.
 [6] S. Fang and E. Kaxiras, Phys. Rev. B **93**, 235153 (2016), URL <https://link.aps.org/doi/10.1103/PhysRevB.93.235153>.
 [7] G. Trambly de Laissardière, D. Mayou, and L. Magaud, Phys. Rev. B **86**, 125413 (2012), URL <https://link.aps.org/doi/10.1103/PhysRevB.86.125413>.
 [8] C. Xu and L. Balents, arXiv:1803.08057 (2018).
 [9] J. F. Dodaro, S. A. Kivelson, Y. Schattner, X.-Q. Sun, and C. Wang, arXiv:1804.03162 (2018).
 [10] M. Fidrysiak, M. Zegrodnik, and J. Spalek, arXiv:1805.01179 (2018).
 [11] H. C. Po, L. Zou, A. Vishwanath, and T. Senthil, arXiv:1803.09742 (2018).
 [12] N. F. Q. Yuan and L. Fu, arXiv:1803.09699 (2018).
 [13] X. Y. Xu, K. T. Law, and P. A. Lee, arXiv:1805.00478 (2018).
 [14] R. Shankar, Rev. Mod. Phys. **66**, 129 (1994), URL <https://link.aps.org/doi/10.1103/RevModPhys.66.129>.
 [15] A. V. Chubukov, S. Sachdev, and T. Senthil, Nuclear Physics B **426**, 601 (1994), ISSN 0550-3213, URL <http://www.sciencedirect.com/science/article/pii/0550321394>.
 [16] P. Hasenfratz and F. Niedermayer, Physics Letters B **268**, 231 (1991), ISSN 0370-2693.
 [17] S. Sachdev, *Quantum Phase Transitions* (Cambridge University Press, 2011).
 [18] S. Hikami and T. Tsuneto, Progress of Theoretical Physics **63**, 387 (1980).
 [19] D. Friedan, Phys. Rev. Lett. **45**, 1057 (1980), URL <https://link.aps.org/doi/10.1103/PhysRevLett.45.1057>.
 [20] D. H. Friedan, Annals of Physics **163**, 318 (1985), ISSN 0003-4916, URL <http://www.sciencedirect.com/science/article/pii/0003491685>.
 [21] H. Isobe, N. F. Q. Yuan, and L. Fu, arXiv:1805.06449 (2018).